Supporting Information

Photoluminescent diamond nanoparticles for cell labelling: study of their uptake mechanism in mammalian cells

O. Faklaris, V. Joshi, T. Irinopoulou, P. Tauc, M. Sennour, H. Girard, C. Gesset, J.-C. Arnault, A. Thorel, J.-P. Boudou, P.A. Curmi, and F. Treussart*

*Laboratoire de Photonique Quantique et Moléculaire, Ecole Normale Supérieure de Cachan and CNRS UMR 8537, Cachan, France (email: francois.treussart@ens-cachan.fr)

Home-built scanning microscope

The **home-built confocal microscope** used to study nanodiamonds photoluminescence with high sensitivity is depicted on **Figure S1**. It relies on a Nikon TE300 stand, equipped with a closed loop piezoelectric three-axis scanning stage (*Tritor 102*, Piezojena, Germany). The excitation beam comes from a cw laser system emitting at a wavelength of 488 nm (*Sapphire 488-50 LP*, Coherent Inc., USA). After its reflection on the dichroic mirror DM (*Q530DCLP*, Chroma Technology Corp., USA), the laser beam is focused onto the sample by an oil immersion objective (Nikon Apochroma, ×60, NA=1.4). The fluorescence is collected by the same objective, forming a collimated beam which then goes through the 200 mm focal length microscope lens tube (LT).

Considering the microscope objective specifications, the Airy disk diameter (distance between the two first minima) in the microscope imaging plane (at the bottom of the stand) is equal to
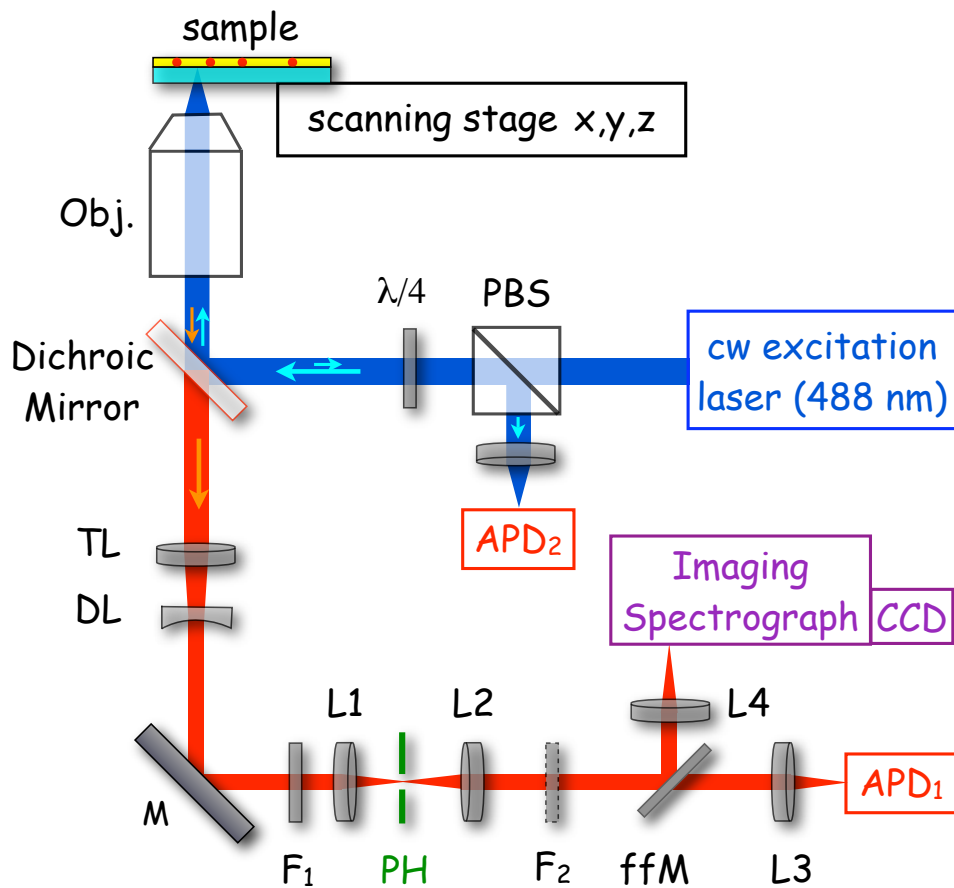
Figure **S1**: Home-built scanning confocal microscopy setup for the study (i) of the photoluminescence of NV color centers in diamond nanocrystals at the single-emitter sensitivity (detection on single-photon counting module APD_1), and (ii) for the simultaneous record of the excitation laser backscaterred light (on detector APD_2).

30 μm. However, we modified the microscope in order to get a collimated beam at its output port. This modification consists in the addition of a diverging lens DL (focal length: -125 mm) after the lens tube turning the beam back into a collimated one, easier to handle for further propagation. The collimated output beam is then focused by the L1 lens (100 mm focal length) into the pinhole (PH). The addition of these two lenses (DL and L1) results in an increase in Airy disk size from 30 to 50 μm which is why we selected a 50 μm diameter pinhole. The residual excitation laser light is removed with the high-pass filter (F_1) having a transmission of 97% in the range 521-1160 nm

(*RazorEdge LP02-514RU-25*, Semrock, USA), before focusing of the signal onto the avalanche photodiode APD_1 in the single-photon counting regime (Single Photon Counting Module, *SPCM-AQR14*, Perkin-Elmer, Canada). An additional filter (F_2) was added in colocalization studies to select either the fluorescence from FITC-labeled endosomes (500-550 nm bandpass filter *ET525-50m*, Chroma Technology Corp., USA), or from the NV color centers ($\lambda > 580$ nm longpass filter, *HQ580LP*, Chroma). Both filters have a flat transmission higher than 97% in the region of interest.

The photoluminescence spectrum of Figure 5d is acquired with an imaging spectrograph (beam intercepted with a flip-flop Mirror (ffM)), simply relying on a concave grating (30% maximum efficiency in its first diffraction order) coupled to a cooled CCD array (back-illuminated *DU-420-BV* detector, Andor Technology, Ireland). The spectral response of the optical elements and of the CCD chip are mostly flat in the 500-750 nm range.
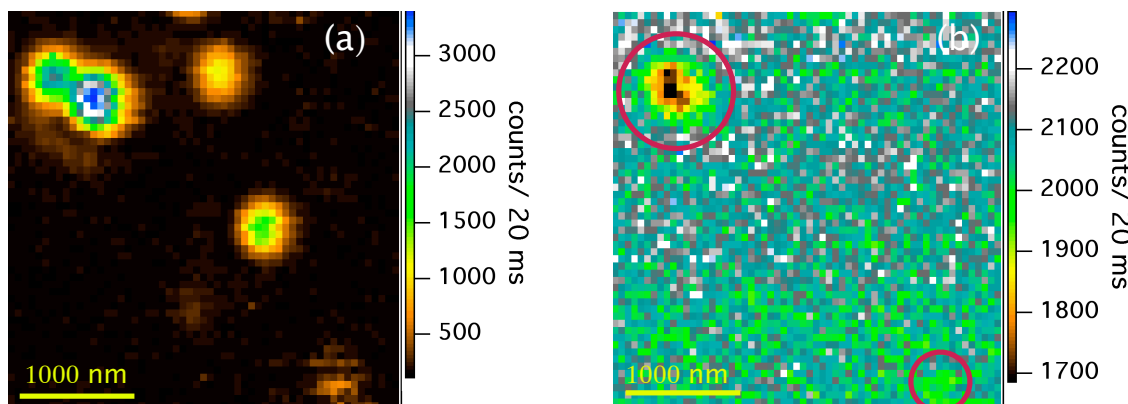

Figure **S2**: Comparison of the photoluminescence and the backscatterred signals coming from PNDs deposited on a glass coverslip, as observed with the home-built scanning microscope. (a) Photoluminescence, (b) back-scattered signal of the same region; encircled in red are PNDs observed in both scans.

In order to image the backscattered light efficiently, the incident beam is circularly polarized[1] with the combination of a polarizing beam-spiltter (PBS) and a quarter-wave plate ($\lambda/4$). After its reflection at the sample coverslip air(or fixation medium)-glass interface, the 488 nm beam

---

[1]Note that an excitation beam circularly polarized is also better suited to excite most of the color centers whatever their absorption dipole orientation is in the sample plane.

helicity is reversed so that the reflected beam is entirely redirected by the PBS on its side port and finally focused on the avalanche photodiode APD_2 (Single Photon Counting Module, *id100-20*, idQuantique, Switzerland). The nanoparticle present on the coverglass surface scatters the excitation laser beam, resulting in a decrease of the reflected light and a signal appearing as a dark spot (as can be seen on **Figure S2b**). The bigger PNDs (or aggregates) are observed in both photoluminescence (**Figure S2a**) and reflection scans, while for the smaller particles (size<40 nm) the back-scattered signal is too weak to be detected but the photoluminescence still yields a strong signal.

Interaction of nanodiamonds with HeLa cells

Cellular uptake dynamics

Figure S3 displays the dynamics of the cellular uptake of PNDs in normal culture conditions.
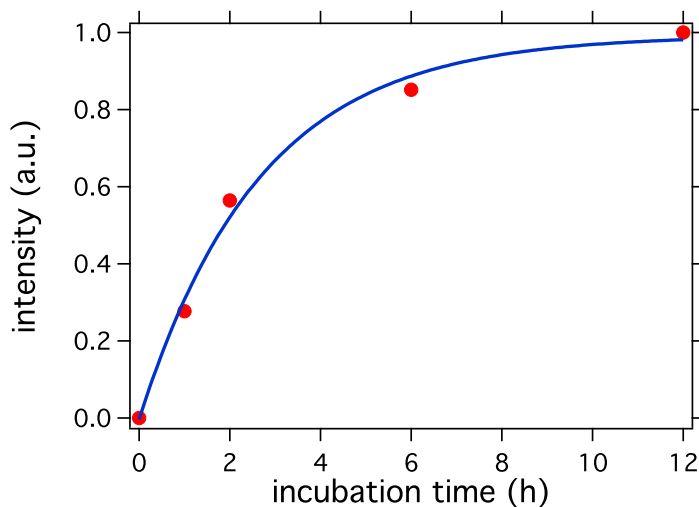

Figure **S3**: Dynamics of photoluminescent nanodiamonds uptake by HeLa cells. The uptake efficiency is quantified by the mean pholuminescence intensity per cell, inferred from confocal imaging in the NV color-center emission spectrum region. This intensity is normalized to one at 12 hours incubation time. Blue solid curve is an exponential fit with a characteristic time of 2.6 hours.

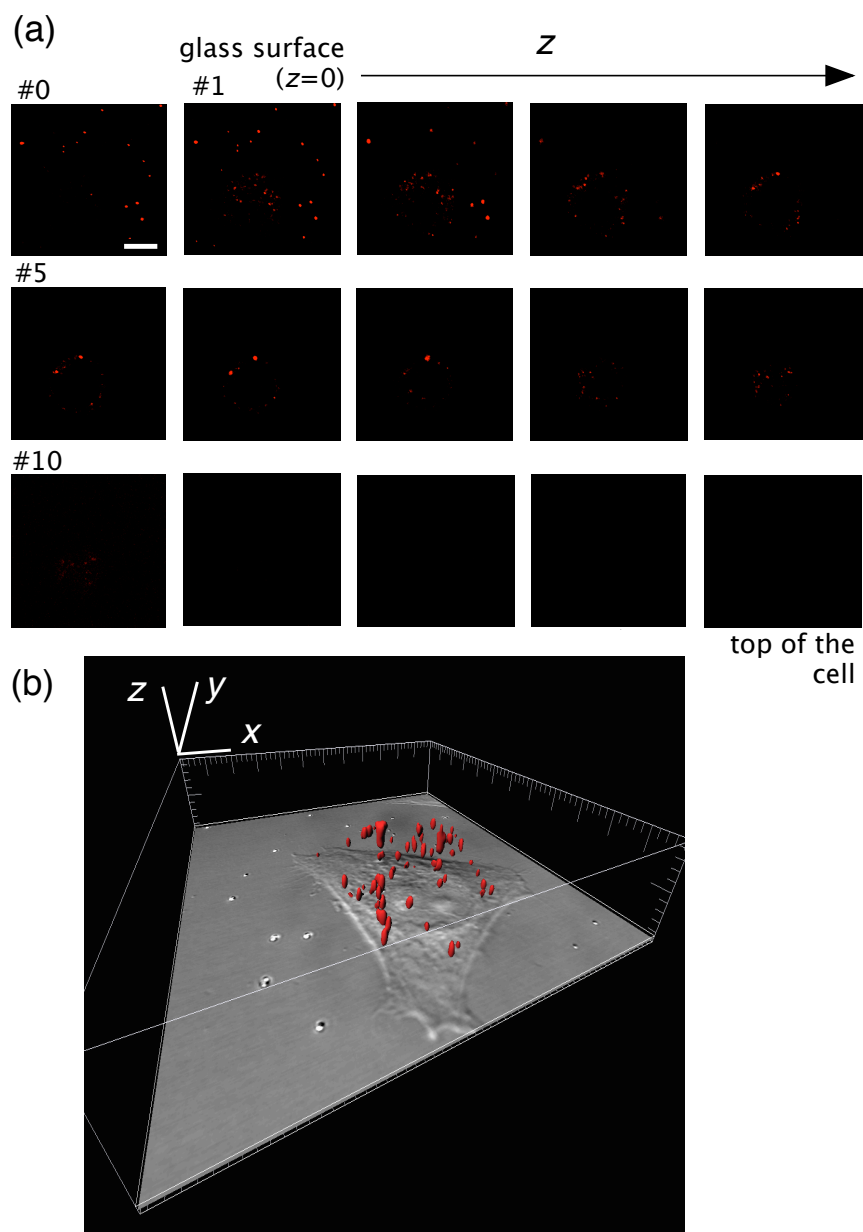# Confocal 3D fluorescence imaging of internalized PNDs in HeLa cells

Figure S4: Three dimensional localization of PNDs in the HeLa cell from Figure 1 (main text). (a) Photoluminescence cross-sections of the cell done with the Leica TCS SP2 fluorescence confocal microscope (in the same conditions as for Fig. 1), at increasing z focusing positions, from the coverglass mounting medium interface ($z = 0$, image #1) on which the cells are grown (upper left scan), to the top of the cell culture ($z \approx 8.9\ \mu$m, bottom right scan).Vertical displacement steps between consecutive scans: 632 nm (image #0 is recorded at $z = -632$ nm); white bar scale: 10 μm. (b) 3-D reconstruction of PNDs spatial distribution. The DIC image of the cell (Fig. 1d) is reproduced in the coverglass plane to localize the PNDs relative to the cell borders. The white bars indicating the 3-axis (x, y, z) orientations have a 10 μm length.

To ensure that PNDs were inside the cell displayed on Figure 1, we performed vertical cross-section scans with the Leica TCS SP2 fluorescence confocal microscope. These scans are displayed on **Figure S4**, with a 3D-reconstruction inferred from this stack of images, using the software *Imaris* (Bitplane, Switzerland). The internalized PNDs appear in the cytoplasm perinuclear region in agreement with previous reports[1–3].
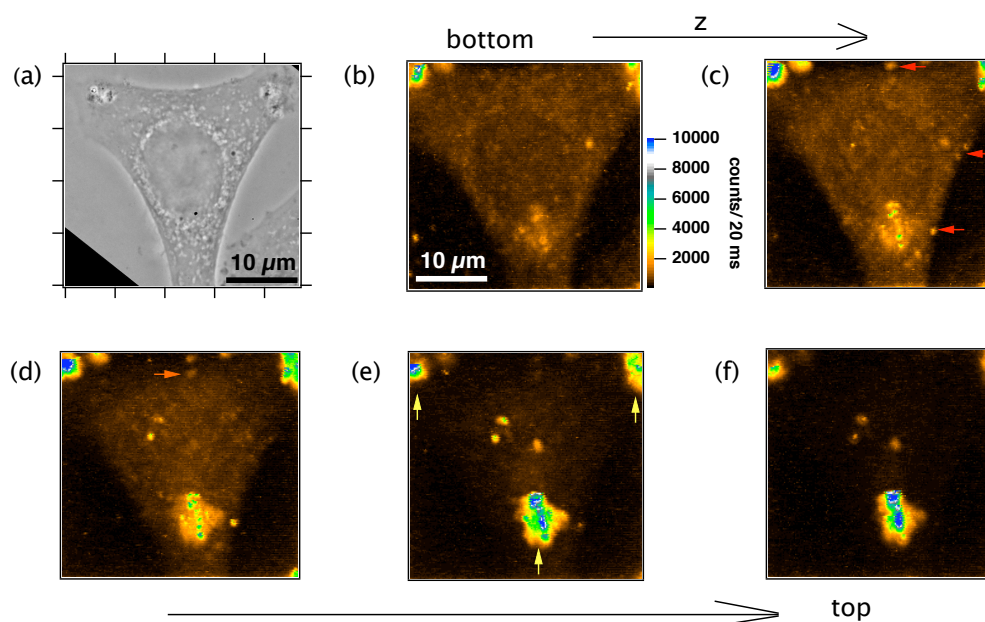
Endocytosis blockage at 4°C

Figure **S5**: Photoluminescence confocal raster-scans of a HeLa cell incubated with PNDs at 4°C. (a) Phase contrast image of the cell under study. (b)-(f) A series of confocal raster scans done with the home-built microscope, at different focusing positions (1 μm displacement step between consecutive scans), from the bottom (coverglass plane, upper left) to the top of the cell (bottom right). Yellow arrows on scan (e) indicate PND-aggregates that are not internalized; red arrows on scan (c) show single PNDs that stay on the membrane; the orange arrow on scan (d) shows the only PND which was internalized.

In order to check that low temperature blocks PNDs internalization even for the smallest particles that cannot be detected on the Leica TCS SP2 microscope, we used the home-built confocal microscope able to detect the smallest PNDs, containing even a single NV center. **Figure S5** shows

a series of confocal cross sections of one HeLa cell. The cells were first incubated with PNDs at 4°C and then fixed. We clearly see that almost no PNDs are present in the cytoplasm. The only ones observed are either on top of the cell, appearing as large aggregates (**Figure S5d-f**), or on the cell membrane as individual particles or small aggregates (**Figure S5c**).

Nanodiamonds and endosomes colocalization

Checking for the absence of crosstalk between channels in colocalization experiments
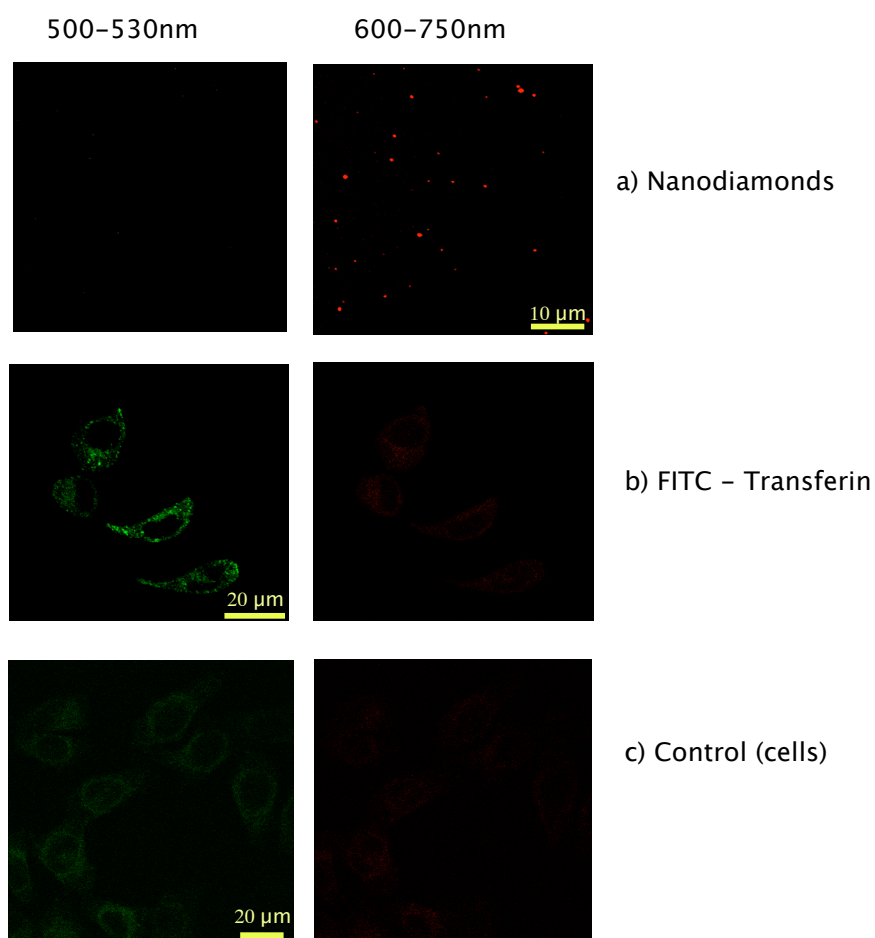

Figure **S6**: Control of the absence of crosstalk between red and green detection channels of the Leica TCS SP2 confocal microscope used for colocalization studies. (a) Raster scan of PNDs deposited on a coverglass, detectable in the red channel only; (b) transferrin - FITC conjugate, internalized in HeLa cells, detectable in the green channel but not in the red; (c) Control cell with no markers, showing the cell autofluorescence.

For the colocalization experiments, we first checked that there is no crosstalk between the different fluorescence detection channels that could lead to artificial colocalization.

We avoided such crosstalk by selecting well separated spectral ranges for the green (500-530 nm, FITC and LysoTracker green dye detection) and red (600-750 nm, NV color centers detection) channels. **Figure S6** shows that there is no signal simultaneously detected in both channels for samples containing only PNDs or only FITC. **Figure S6** also displays the autofluorescence signal of cells, detectable in the green but not in the red channel. Similar selective filtering was ensured by filter F_2 on the home-built confocal microscope (**Figure S1**).

PNDs-endosomes colocalization study with the home-built confocal microscope

PNDs-endosomes colocalization was studied at the single particle and single color-center sensitivity levels for this type of PNDs, similarly to previously reported work using PNDs prepared differently[1]. **Figure S7** shows that 7 PNDs out of 26 internalized in the cell are colocalized with endosomes, which is a proportion similar to the previous report[1].
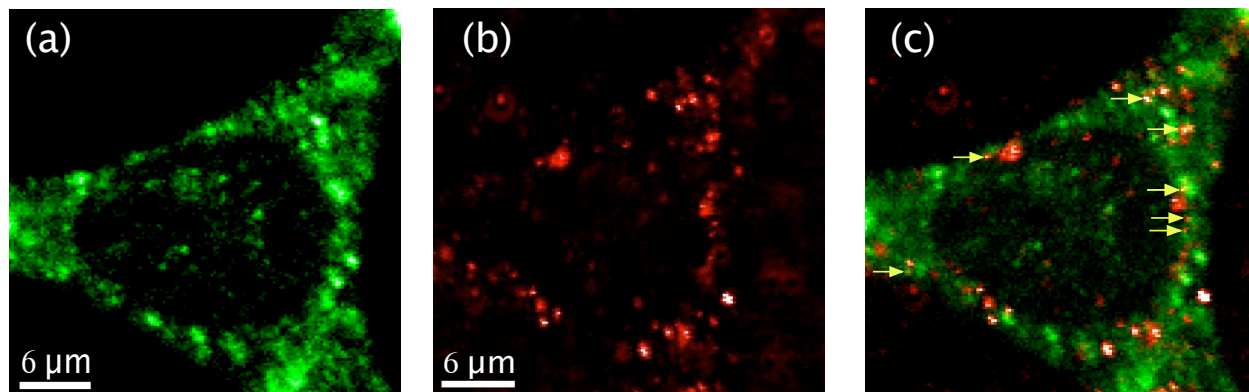

Figure **S7**: Colocalization of PNDs with endosomes observed with the home-built confocal microscope. (a) Confocal raster-scan in the green detection channel (filter F_2: bandpass 500-550 nm) showing early endosomes labeled by EEA1-FITC conjugate; (b) photoluminescence raster scan in the red channel (filter F_2: longpass $\lambda > 580$ nm), showing PNDs; (c) Merged image of (a) and (b) scans, with arrows showing PNDs colocalized with endosomes; raster scans recorded 1.5 μm above the coverglass surface, laser excitation wavelength 488 nm, power 0.4 mW.

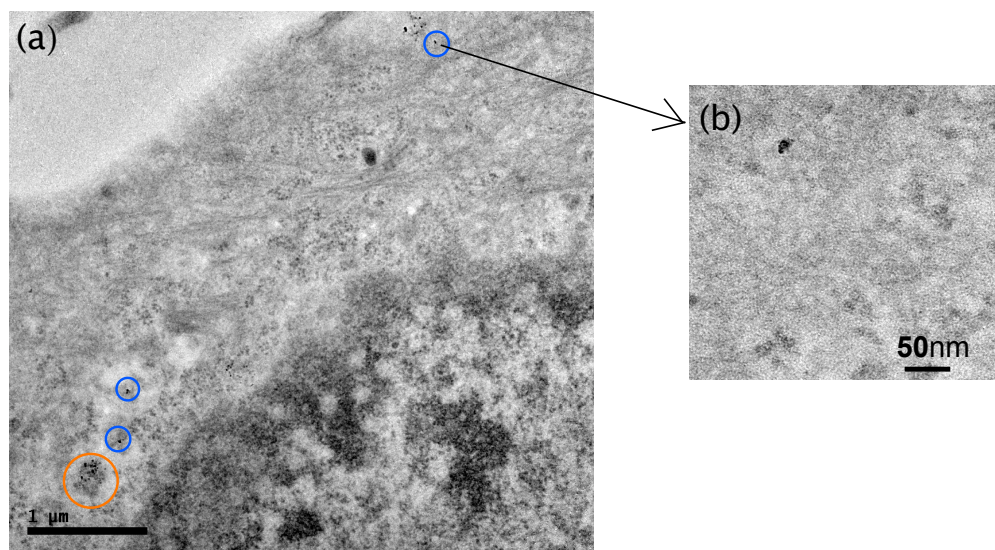**Additional High Resolution TEM image of PNDs in HeLa cell**

Figure **S8**: High-Resolution TEM Images of a HeLa cell incubated with PNDs. (a) large scale image displaying part of the nucleus in the bottom right. Nanodiamonds trapped in a vesicles are circled in orange. Blue circles indicate nanoparticles being free in the cytosol. (b) zoom on one of these nanoparticles, of size $\simeq$ 10 nm. Scale bar on (a): 1 μm.

Figure S8 shows additional HR-TEM images. The sample is the same as the one used for Figure 4. Some nanodiamonds appear as aggregates accumulated in endocellular vesicles (marked with an orange circle) but a significant portion of PNDs stays **free in the cytosol** (blue circles).

Surface characterization of PNDs in serum supplemented culture medium

The Fœtal Calf Serum (FCS) was used to supplement DMEM cell culture medium allowing normal cell growth. It contains a diverse set of proteins, like bovine serum albumin (BSA), transferrin, α- and β- globulin, etc...BSA being the dominant protein. We have strong indications that NDs uptake is receptor mediated. Such mechanism is usually influenced by the chemical functions present at the nanodiamond surface.

We therefore carried out Fourier Transport InfraRed (FT-IR) spectal analysis of the nanodiamonds after their interaction with the serum supplemented culture medium. This interaction

leads to NDs surface function changes compared to their surface in aqueous suspension, due for example to nonspecific **adsorption of serum proteins**. Such binding could **enhance the receptor-mediated endocytosis mechanism**, as found recently for gold nanoparticles[4].

Zeta potential measurements

To check whether the serum proteins can be adsorbed on PNDs surface, we measured the ζ-potential of nanodiamonds initially incubated with culture medium supplemented with fœtal calf serum. Acid-treated PNDs (1 mg) were incubated with DMEM containing 10% FCS and sonicated for about 15 min. After two hours of incubation at room temperature and vortexing, the solution was washed by three successive centrifugations to eliminate the excess of proteins and then redispersed in pure water. The obtained PNDs aqueous suspensions exhibited a zeta potential $\zeta = -15,6$ mV (at pH=7), corresponding to a 2.5 fold decrease compared to pristine PNDs, which is a consequence of the change of its surface functions. This result agrees with previous studies, in which BSA was used as a stabilizer for Al_2O_3 or gold nanoparticles aqueous colloidal suspensions and where a similar change of the ζ-potential was observed[5,6]. The suspension remained stable for many hours after the initial mixture. After a few days we observed the formation of some aggregates (confirmed by DLS measurements) which could be redispersed to the primary particles by sonication.

It is also worth to note that when PNDs are added to DMEM without serum they strongly aggregate within one hour (to micron size aggregates), most probably due to the high ionic strength of DMEM leading to the screening of the NDs mutual electrostatic repulsion. On the contrary if one supplements DMEM with FCS, PNDs do not aggregate on a few hours timescale.

FT-IR spectroscopy measurement

To check for the presence of adsorbed serum proteins on PNDs we performed FT-IR spectroscopy measurements. The PNDs-proteins sample was mixed with KBr powder and pressed into pellets

which were then placed in an IR cell. The FT-IR spectra of the KBr pellets were recorded with a FT-IR spectrometer (*Nicolet 8700 Research FT-IR*, Thermo Fisher Scientific Inc., USA) under a continuous flow of nitrogen gaz to avoid water adsorption on the sample.
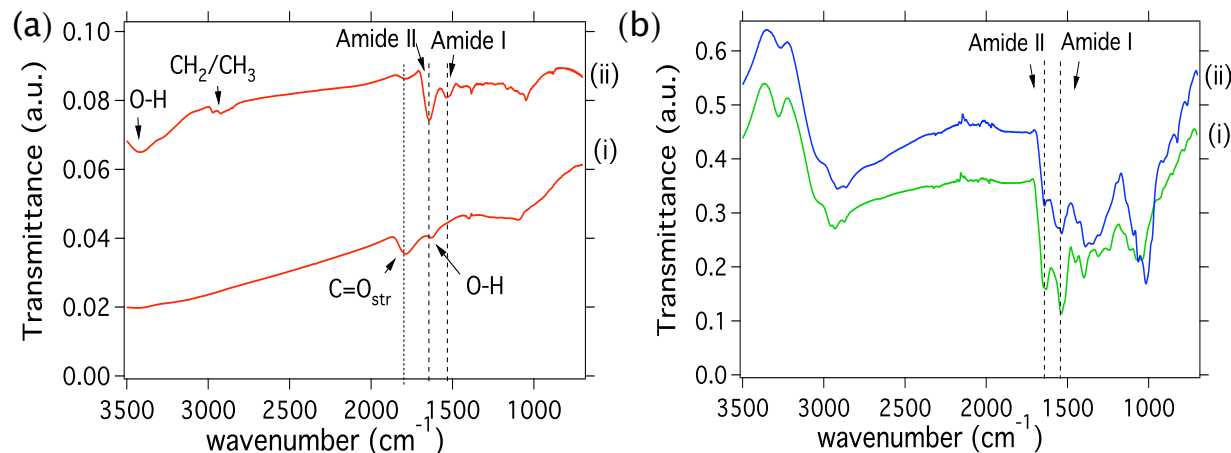

Figure **S9**: Infrared spectroscopic study of surface functions present on nanodiamonds after incubation with serum supplementted culture medium. (a) FT-IR spectra of nanodiamonds after incubation with fœtal calf serum supplemented cell culture medium: (i) pristine PNDs ; (ii) PNDs-serum proteins conjugates; (b) FT-IR spectra of serum proteins: (i) spectrum of DMEM medium containing 10% foetal calf serum (FCS); (ii) spectrum of pure FCS solution.

Results and discussion

The transmission FT-IR spectrum of pristine PNDs (**Figure S10a(i)**) shows a band near 1775 cm^{-1} which can be attributed to the C=O stretching mode of the carboxylic acid groups, and a weak band near 1630 cm^{-1} that can be assigned to the O-H bending of the same groups on the ND surface[7,8]. O-H bending band due to the remaining physically adsorbed water appears at 3400 cm^{-1}.

When nanodiamonds were incubated with serum proteins two new infrared bands appeared, one at 1640 cm^{-1} and the other at 1538 cm^{-1} (**Figure S10a(ii)**). These two bands are due to serum proteins according to the FT-IR spectrum of the serum proteins displayed on **Figure S10b**. The peak near 1640 cm^{-1} represents the amide II band and the peak at 1538 cm^{-1} corresponds to the amide I band[9,10]. Moreover, on the pristine NDs spectrum, the 1775 cm^{-1} band is much weaker after ND interaction with serum proteins. This is due to the relative diminution of the

carboxylic functions on the PND surface consecutive to the adsorption of serum proteins. This phenomenon probably results from electrostatic attraction of positively charged amino groups of the proteins by the negatively charged nanodiamonds.

Finally, an additional proof of serum proteins adsorption on PNDs is the band at 2900 cm^{-1}, which can be attributed to the CH_2/CH_3 groups of the alkyl chain of the proteins[7].

Cytotoxicity tests

A necessary requirement to use PNDs as cell and biomolecule labels is that they should present a low cytotoxicity. **As cytotoxicity depends on the cellular type used and the size, shape and charge of the PNDs**, we performed MTT assays for the type of PNDs used in this work.
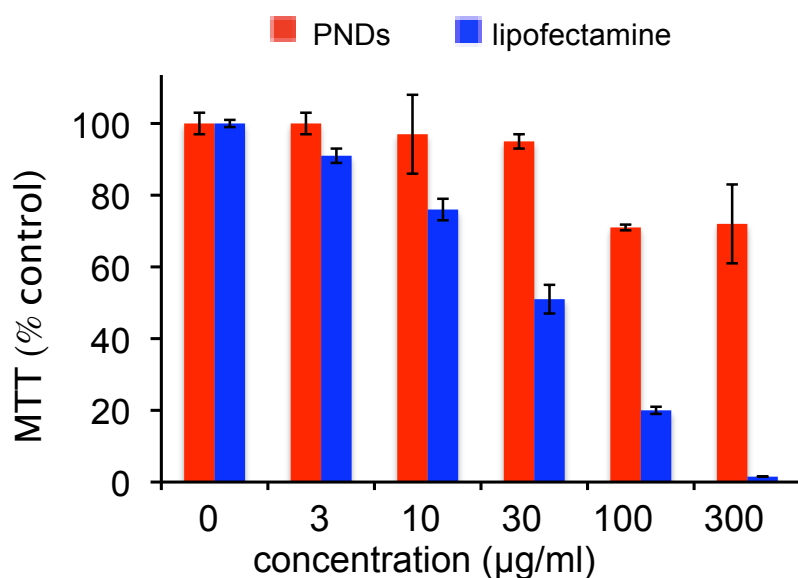

Figure **S10**: MTT cytotoxicity assay performed after 24 h incubation of HeLa cells with PNDs and lipofectamine. PNDs seem to be non toxic, in contrast to lipofectamine which appears to be toxic for concentrations $> 10\,\mu$g/ml.

Cells were plated at a concentration of 2×10^5 cells/1.3 cm^2 for 24 h and then treated with various concentrations of PNDs for 24 h in 10% serum supplemented medium. We conducted the MTT assay (3-[4,5 -thylthiazol- 2-yl]-2,5-diphenyl-tetrazolium bromide) relying on mitochondrial

12

activity measurement to assess cellular viability [11]. A purple color developed within the cells after 2 h of incubation with MTT indicates the cleavage of the tetrazolium salt (MTT) by mitochondrial reductance in live cells. The purple formazan crystals are then dissolved in acidified isopropanol and the absorbance of the solution is measured with a spectrophotometer (*Uvikon XL*, Secoman, France) at 570 nm. The absorbance of cells exposed to PNDs was compared to control cells, not exposed to PNDs, which is associated to 100% absorbance. As a positive control we used Lipofectamine (Invitrogen, USA), a substance widely used for cell transfections, but considered as toxic for long exposition times and doses.

Figure S10 presents the survival rate as measured with MTT assay for the PNDs used in our experiments. We observed that **PNDs do not induce cell death** at low doses, and at high doses they appear to be less toxic than lipofectamine.

References

1. Faklaris, O.; Garrot, D.; Joshi, V.; Druon, F.; Boudou, J.; Sauvage, T.; Georges, P.; Curmi, P.; Treussart, F. Detection of single photoluminescent diamond nanoparticles in cells and study of their internalization pathway. *Small* **2008**, *4*, 2236–2239.

2. Fu, C.-C.; Lee, H.-Y.; Chen, K.; Lim, T.-S.; Wu, H.-Y.; Lin, P.-K.; Wei, P.-K.; Tsao, P.-H.; Chang, H.-C.; Fann, W. Characterization and applications of single fluorescent nanodiamonds as cellular biomarkers. *Proc. Nat. Acad. Sc.* **2007**, *104*, 727.

3. Chao, J.-I.; Perevedentseva, E.; Chung, P.-H.; Liu, K.-K.; Cheng, C.-Y.; Chang, C.-C.; Cheng, C.-L. Nanometer-Sized Diamond Particle as a Probe for Biolabeling. *Biophys. J.* **2007**, *93*, 2199.

4. Chithrani, B.; Ghazani, A.; Chan, W.-C. Determining the Size and Shape Dependence of Gold Nanoparticle Uptake into Mammalian Cells. *Nano Lett.* **2006**, *6*, 662– 668.

5. Rezwan, K.; Meier, L.; Rezwan, M.; Voros, J.; Textor, M.; Gauckler, L. Bovine Serum Albumin Adsorption onto Colloidal Al_2O_3 Particles: A New Model Based on Zeta Potential and UV-Vis Measurements. *Langmuir* **2004**, *20*, 10055–10061.

6. Brewer, S. H.; Glomm, W.; Johnson, M.; Knag, M.; Franzen, S. Probing BSA Binding to Citrate-Coated Gold Nanoparticles and Surfaces. *Langmuir* **2005**, *21*, 9303–9307.

7. Chung, P.-H.; Perevedentseva, E.; Tu, J.-S.; Chang, C.-C.; Cheng, C.-L. Spectroscopic study of bio-functionalized nanodiamonds. *Diamond Relat. Mater.* **2005**, *15*, 622.

8. Vial, S.; Mansuy, C.; Sagan, S.; Irinopoulou, T.; Burlina, F.; Boudou, J.; Chassaing, G.; Lavielle, S. Peptide-grafted nanodiamonds: preparation, cytotoxicity and uptake in cells. *ChemBioChem* **2008**, *9*, 2113–2119.

9. Militello, V.; Casarino, C.; Emanuele, A.; Giostra, A.; Pullara, F.; Leone, M. Aggregation kinetics of bovine serum albumin studied by FTIR spectroscopy and light scattering. *Bioph. Chem.* **2004**, *107*, 175187.

10. Murayama, K.; Tomida, M. Heat-Induced Secondary Structure and Conformation Change of Bovine Serum Albumin Investigated by Fourier Transform Infrared Spectroscopy. *Biochem.* **2004**, *43*, 11526–11532.

11. Carmichael, J.; DeGraff, W.; Gazdar, A.; Minna, J.; Mitchell, J. Evaluation of a Tetrazolium-based Semiautomated Colorimetric Assay: Assessment of Chemosensitivity Testing. *Cancer Res.* **1987**, *47*, 936–942.